Report Documentation Page

Public reporting burden for the collection of information is estimated to average 1 hour per response, including the time for reviewing instructions, searching existing data sources, gathering and maintaining the data needed, and completing and reviewing the collection of information. Send comments regarding this burden estimate or any other aspect of this collection of information, including suggestions for reducing this burden, to Washington Headquarters Services, Directorate for Information Operations and Reports, 1215 Jefferson Davis Highway, Suite 1204, Arlington VA 22202-4302. Respondents should be aware that notwithstanding any other provision of law, no person shall be subject to a penalty for failing to comply with a collection of information if it does not display a currently valid OMB control number.

1. REPORT DATE **01 SEP 2013**	2. REPORT TYPE **N/A**	3. DATES COVERED **-**

4. TITLE AND SUBTITLE	5a. CONTRACT NUMBER
Low-dose CT for quantitative analysis in acute respiratory distress syndrome.	5b. GRANT NUMBER
	5c. PROGRAM ELEMENT NUMBER

6. AUTHOR(S)	5d. PROJECT NUMBER
Vecchi V., Langer T., Bellomi M., Rampinelli C., Chung K.K., Cancio L.C., Gattinoni L., Batchinsky A.I.,	5e. TASK NUMBER
	5f. WORK UNIT NUMBER

7. PERFORMING ORGANIZATION NAME(S) AND ADDRESS(ES) **United States Army Institute of Surgical Research, JBSA Fort Sam Houston, TX**	8. PERFORMING ORGANIZATION REPORT NUMBER

9. SPONSORING/MONITORING AGENCY NAME(S) AND ADDRESS(ES)	10. SPONSOR/MONITOR'S ACRONYM(S)
	11. SPONSOR/MONITOR'S REPORT NUMBER(S)

12. DISTRIBUTION/AVAILABILITY STATEMENT
Approved for public release, distribution unlimited

13. SUPPLEMENTARY NOTES

14. ABSTRACT

15. SUBJECT TERMS

16. SECURITY CLASSIFICATION OF:			17. LIMITATION OF ABSTRACT	18. NUMBER OF PAGES	19a. NAME OF RESPONSIBLE PERSON
a. REPORT **unclassified**	b. ABSTRACT **unclassified**	c. THIS PAGE **unclassified**	**UU**	**27**	

Low-dose CT for quantitative analysis in acute respiratory distress syndrome

Vittoria Vecchi [1,2,4*], Thomas Langer [1,3,4*], Massimo Bellomi [2,5], Cristiano Rampinelli [5],

Kevin K. Chung [1], Leopoldo C. Cancio [1], Luciano Gattinoni [3,6] and Andriy I. Batchinsky [1]

[1] US Army Institute of Surgical Research, Fort Sam Houston, San Antonio, TX

[2] School of Medicine, Università degli Studi di Milano, Milan, Italy

[3] Dipartimento di Fisiopatologia medico-chirurgica e dei trapianti; Università degli Studi di Milano, Milan, Italy

[4] National Research Council, National Academies, Washington DC

[5] Department of Radiology, European Institute of Oncology, Milan, Italy

[6] Dipartimento di Anestesia, Rianimazione (Intensiva e Sub-intensiva) e Terapia del Dolore, Fondazione IRCCS Ca'

Granda Ospedale Maggiore Policlinico di Milano, Milan, Italy

* contributed equally to the study.

Corresponding author:

Thomas Langer, MD
Dipartimento di Fisiopatologia medico-chirurgica e dei trapianti;
Università degli Studi di Milano
Via F. Sforza 35, 20122 Milano, Italy
Phone: +39 02 55033232
Fax: +39 02 55033230
E-mail: thomas.langer@unimi.it

Abstract

Introduction: The clinical use of serial quantitative computed tomography (CT) to characterize lung disease and guide the optimization of mechanical ventilation in patients with acute respiratory distress syndrome (ARDS) is limited by the risk of cumulative radiation exposure and by the difficulties and risks related to transferring patients to the CT room. We evaluated the effects of tube current-time product (mAs) variations on quantitative results in healthy lungs and in experimental ARDS in order to support the use of low-dose CT for quantitative analysis.

Methods: In 14 sheep chest CT was performed at baseline and after the induction of ARDS via intravenous oleic acid injection. For each CT session, two consecutive scans were obtained applying two different mAs: 60 mAs was paired with 140, 15 or 7.5 mAs. All other CT parameters were kept unaltered (tube voltage 120 kVp, collimation 32x0.5 mm, pitch 0.85, matrix 512x512, pixel size 0.625x0.625 mm). Quantitative results obtained at different mAs were compared via Bland-Altman analysis.

Results: Good agreement was observed between 60 mAs and 140 mAs and between 60 mAs and 15 mAs (all biases less than 1%). A further reduction of mAs to 7.5 mAs caused an increase in the bias of poorly and non aerated tissue (-2.9 and 2.4%, respectively) and determined a significant widening of the limits of agreement for the same compartments (-10.5 - 4.8 % for poorly aerated and -5.9 - 10.8% for non aerated tissue). Estimated mean effective dose at 140, 60, 15 and 7.5 mAs corresponded to 17.8, 7.4, 2.0 and 0.9 *millisievert*, respectively. Image noise of scans performed at 140, 60, 15 and 7.5 mAs corresponded to 10, 16, 38 and 74 Hounsfield Units, respectively.

Conclusions: A reduction of effective dose up to 70% has been achieved with minimal effects on lung quantitative results. Low-dose computed tomography provides accurate quantitative results and could be used to characterize lung compartment distribution and possibly monitor time-course of ARDS with a lower risk of exposure to ionizing radiation. A further radiation dose reduction is associated with lower accuracy in quantitative results.

Introduction

Chest computed tomography (CT) and the related lung quantitative analysis (qCT) have greatly improved the understanding of the pathophysiological and morphological features of the acute respiratory distress syndrome (ARDS) [1-6]. Moreover, qCT has been proposed as a valuable tool to determine the potential for lung recruitment (thus optimizing the setting of positive end-expiratory pressure [7]) and to assess lung opening and closing as well as lung hyperinflation in order to reduce the occurrence of ventilator-induced lung injury [8,9].

Besides from the difficulties and risks related to transferring patients to the CT room, one of the major factors hindering the adoption of serial qCT is the associated patient exposure to ionizing radiation [10-12]. Radiation dose is linearly related to the tube current-time product (mAs) which affects the image noise level and thus influences image quality [13]. In general, an increase in mAs will improve image quality at the cost of a higher radiation dose, while a reduction in mAs will have the opposite effect [14], but other factors may be implied, such as tissue-weighting, use of automatic tube current modulation technique or variations in kVp between others.

It is worth mentioning that, despite the extensive use of qCT, a standardized protocol for the acquisition parameters of CT images has not been defined and, in particular, widely variable mAs have been reported both in experimental [15,16] and clinical settings [17,18].

While low dose CT has been extensively used in other fields [19-21], limited data are available on its application for lung quantitative analysis. Indeed, aside from a few studies on pulmonary emphysema [22-24], that showed that quantification of hyperinflated tissue is not affected by a reduction of tube current-time product to 20 mAs [22], no data are available on the possible effects of different mAs on quantitative lung analysis results.

If quantitative results performed on low- to ultra low-dose chest CT scans were accurate, qCT could be used more frequently to characterize lung compartment distribution and potential for lung recruitment with a reduced radiation exposure. The aim of the present study was therefore to investigate the effects of variations in mAs on quantitative results in healthy lungs and in experimental ARDS.

Materials and methods

This study was approved by the US Army Institute of Surgical Research Animal Care and Use Committee and was conducted in compliance with the Animal Welfare Act, the implementing Animal Welfare Regulations and in accordance with the principles of the Guide for the Care and Use of Laboratory Animals.

Fourteen anesthetized and mechanically ventilated female sheep (44±6 kg, 1-2 years of age) were studied. All animals were included in other protocols conducted at the US Army Institute of Surgical Research (i.e., no animal was used for the sole purpose of this study). Further details are provided in the Electronic Supplementary Material.

CT scan image acquisition and reconstruction

Chest CT (Toshiba Aquilion 64-slice Medical System, Tustin, CA) was performed at baseline (healthy lungs) and 6-8 hours after the induction of ARDS. Experimental ARDS was induced via intravenous injection of 0.1-0.15 ml/kg of oleic acid [25].

Before scanning, the degree of inflation of the cuff of the endotracheal/tracheostomy tube was checked in order to minimize/avoid the possible air leakage. During CT image acquisition, two consecutive scans were performed after having clamped the endotracheal/tracheostomy tube during a respiratory hold performed with the mechanical ventilator (Servo 300, Siemens, Solna, Sweden). The entire lung was imaged. For each couple of scans two different mAs were applied in randomized order to compare the corresponding quantitative results: 60 mAs was chosen as

reference value according to the weight range of studied animals [26,27] and was paired with 140, 15 or 7.5 mAs. Each couple of scans, acquired at the same airway pressure during a respiratory hold, consisted therefore of a scan performed at 60 mAs and a scan performed either at 140, 15 or 7.5 mAs. All other CT parameters were kept unaltered (tube voltage 120 kVp, rotation time 0.5 s, collimation 32x0.5 mm, pitch 0.85, reconstruction matrix 512x512, pixel size 0.625x0.625 mm). Automatic tube current modulation technique was not applied during scan acquisition. Images were reconstructed using a 5-mm section width, a 5-mm interval and a body standard axial filter (FC13).

Quantitative analysis

Images were processed with an image-analysis software (Maluna 3.17, Göttingen, Germany). The pulmonary tissue was selected as previously described [28]. Briefly, lung boundaries were drawn automatically on each baseline image and manually on each CT image acquired on sheep with experimental ARDS. After processing each slice of a series, total lung volume, total lung tissue mass and frequency distribution of lung CT numbers expressed in Hounsfield Units (HU) were computed. Based on their degree of aeration, four different lung compartments were quantified, according to usual thresholds [3]: hyperinflated tissue (-1000 to -901 HU), normally aerated tissue (-900 to -501 HU), poorly aerated tissue (-500 to -101 HU) and non aerated tissue (-100 to +200 HU).

Dose and noise evaluation.

Volumetric computed tomography dose index ($CTDI_{vol}$) and dose length product (DLP) of each scan were recorded as reported by the CT scanner. Effective dose (E) was estimated using the DLP method [29]. Image noise levels for each applied mAs were calculated as the mean standard deviation (SD) of tissue density in a uniform area (within the aorta) of ten different scans [30].

Statistical analysis

Data are expressed as mean ± SD, unless otherwise stated. Results obtained at baseline and after the induction of ARDS were analyzed separately. The agreement between quantitative results obtained

from consecutive scans performed with different mAs was assessed via Bland-Altman analysis [31], linear regression and paired t-test or Signed Rank Sum test, as appropriate. The difference between CT number frequency distribution of the different mAs was assessed via paired t-test or Signed Rank Sum test, as appropriate. One-way analysis of variance was used to compare $CTDI_{vol}$, DLP, E and image noise of the different applied mAs. A rank transformation was used for non-normally distributed variables that did not pass the equal variance test. Statistical significance was defined as $p<0.05$. Statistical analysis was performed with SigmaPlot 11.2 (Systat Software Inc. San Jose, CA).

Results

A total of 218 CT scans were acquired, 92 at baseline and 126 during experimental ARDS. Forty comparisons between 60 and 140 mAs (12 baseline, 28 ARDS), 36 comparisons between 60 and 15 mAs (18 baseline, 18 ARDS) and 33 comparisons between 60 and 7.5 mAs (16 baseline, 17 ARDS) were performed.

The reduction of mAs was associated with an increase in image noise and a worsening of image quality (Figure 1). However, the increased image noise did not hinder the recognition of the interface between lung and surrounding structures.

Both in healthy lungs and during experimental ARDS, excellent agreement was observed between qCT results obtained at 60 and 140 mAs (Table 1), and good agreement between those obtained at 60 mAs and 15 mAs (Table 2). The further reduction of current-time product to 7.5 mAs was associated with a marked increase of bias and limits of agreement of Bland-Altman analysis, in particular for poorly and non aerated lung compartments of sheep with experimental ARDS (Table 3 and Figure 2). Additional Bland-Altman plots of different comparisons are reported in the Electronic Supplementary Material (Additional file 1, Figures E1-6).

Frequency distribution of CT numbers at different mAs in healthy sheep and sheep with experimental ARDS are reported in Figure 3 and Figure 4, respectively. Of note, the reduction of mAs to 7.5 mAs caused significant changes in frequency distribution of CT numbers.

Mean recorded values of $CTDI_{vol}$, DLP, image noise and mean estimated value of E are reported in Table 4. When comparing the mean values of E at 15 mAs (2.0±0.8 *millisievert*) and at 7.5 mAs (0.9±0.1 *millisievert*) to the mean value of E at 60 mAs (7.4±0.9 *millisievert*), a dose reduction of 73% and 88% was respectively achieved. Additional results are provided in the Electronic Supplementary Material.

Discussion

In this study we have shown that a reduction of effective dose up to 70% can be achieved with minimal effects on lung quantitative results and that low dose CT could therefore be a valuable tool to characterize lung compartment distribution and possibly monitor time-course of ARDS with a lower risk of exposure to ionizing radiation.

Quantitative results obtained at 60 mAs were compared both with the results obtained at a higher dose (140 mAs) chosen within the range of doses commonly used for standard chest CT in adults [32] and with the results obtained at two progressively lower doses (15 and 7.5 mAs).

We analyzed both scans performed on healthy sheep and on sheep with experimental ARDS. Overall, the majority of lung tissue (~80%) was normally aerated at baseline, while approximately 90% of lung tissue was poorly or non aerated after the induction of ARDS. On one hand, through the analysis of healthy lungs we aimed at studying the pure physical effects of mAs-related noise variations on the quantitative analysis. Indeed, the interface between healthy pulmonary parenchyma and surrounding structures (i.e., thoracic wall, mediastinum, diaphragm, hilar vessels, main and lobar bronchi) was perfectly recognizable regardless of the applied mAs and the difference between their densities allowed the use of the automated function of the quantitative analysis software to outline the regions of interest. In this group we could therefore safely state that,

within compared scans, equivalent regions of interest were analyzed. On the other hand, when analyzing scans of injured sheep, the possibility of an additional effect had to be taken into account. Indeed, considering the similarity between densities of injured lungs and other thoracic structures, the operator-dependent ability to recognize lung boundaries could have been impaired by the worsening image quality (noisier) of the lower dose images (15 and 7.5 mAs). This in turn could have led to differences in the manual selection of regions of interest within compared scans. In this regard, despite the slight change in image noise (Table 4), image quality did not vary notably between scans performed at 60 and 140 mAs (Figures 1A and 1B). Moreover, although the significant increase in image noise caused a progressive deterioration in image quality, even on scans performed at 15 and 7.5 mAs (Figures 1C and 1D) the recognition of lung and surrounding structures (which is the sole requirement to perform qCT) was preserved.

Both in healthy lungs and in lungs with experimental ARDS, quantitative results obtained at 60 and 140 mAs showed excellent limits of agreement and biases close to 0% and the statistical analysis did not point out any significant difference (Table 1). Also the comparison of qCT data obtained at 60 and 15 mAs (Table 2) showed good limits of agreement and biases lower than 1%. However, a further reduction of mAs to 7.5 caused both an increase in biases and a widening of the limits of agreement, especially for poorly and non aerated lung tissue in sheep with experimental ARDS.

Figures 3 and 4, besides pointing out the evident densitometric change between healthy and injured lungs, show that the mAs reduction increased image noise (Table 4) and thus caused a progressive change in frequency distribution of CT numbers.

Indeed, the comparison of frequency distribution of CT numbers between 60 and 15 mAs and between 60 and 7.5 mAs at baseline (Figures 3B and 3C) showed a progressive shift of tissue from the normally to the hyperinflated compartment related to the reduction in mAs which explains the higher percentages of hyperinflated lung tissue measured with lower doses. Similarly, when

observing the comparison of frequency distribution of CT numbers between 60 and 15 mAs and between 60 and 7.5 mAs during experimental ARDS (Figures 4B and 4C), a progressive shift of tissue from the non aerated to the poorly aerated compartment was measured. Finally, the change in frequency distribution explains also the significant decrease in total lung volume, observed especially at the lowest dose on scans performed during experimental ARDS. Indeed, the observed widening of the frequency distribution of density at 7.5 mAs (Figure 4C) caused a shift of non aerated tissue both toward the poorly aerated compartment (as described above) and toward CT numbers greater than the threshold of +200 HU, commonly used as the upper limit for the non aerated tissue. It is worth mentioning that, for this reason, tissue densities measured as greater than +200 HU were excluded from the overall computation, despite being part of the region of interest. This fact explains the underestimation at 7.5 mAs of total lung volume. Moreover, as part of non aerated tissue is shifted toward CT numbers not included in the overall computation, this effect accounts in part also for the above mentioned reduction of non aerated tissue measured at 7.5 mAs. Of note, the underestimation of total lung volume and (in part) of non aerated tissue could be avoided by increasing the included HU range (e.g., up to +500 HU).

The described effect of image noise level on the frequency distribution of tissue density is also clearly represented when analyzing a region of interest positioned on a uniform tissue (aorta): the progressive reduction of mAs is associated with a lowering of the distribution peak and a corresponding widening of the distribution curve (See Additional File 1, Figure E7).

The establishment of a standardized protocol would prevent any mAs-related difference in quantitative results. Indeed, just as the reconstruction parameters [33], identical acquisition parameters need to be used in order to compare quantitative results of different scans performed on the same patient as well as quantitative results of different studies, scanners and institutions [34]. When defining a standardized CT acquisition protocol for quantitative analysis, the "ALARA concept" (As Low As Reasonably Achievable) [35,36] should be taken into account and our study supports the use of low dose CT for this purpose. Indeed, we may speculate that, at the same

effective dose of 1 scan performed at 140 mAs, approximately 2 scans at 60 mAs or 10 scans at 15 mAs could be performed (Table 4). Moreover, it is worth mentioning that the use of low-dose CT could be coupled with the simplified analysis method based on the extrapolation of whole lung results from ten CT scan slices [37,38]. This, besides shortening the time needed to perform qCT, would allow a further reduction of radiation dose.

As a limitation of the present study we need to point out that the absolute mAs values used in this experimental study cannot be applied directly to patients with ARDS. Indeed, being image noise directly correlated to body weight [39] it is conceivable that such mAs values would be associated to higher image noise that could therefore affect quantitative results significantly.

Finally, the worsening of image quality caused by the reduction of mAs during CT acquisition should be kept in mind as it could limit the diagnostic ability of CT examinations.

Conclusions

A reduction of effective dose up to 70% can be achieved with minimal effects on lung quantitative results. Lung quantitative analysis performed on low dose CT scans provides accurate results both in healthy lungs and in experimental ARDS and is therefore a valuable tool to characterize and potentially monitor lung disease. In particular, if multiple chest CT scans are performed in order to characterize quantitatively the lung and assess the response to the application of different airway pressures (potential for lung recruitment), low dose CT could be used to reduce patient's radiation exposure. This, of course, needs to be proved in the real word of the Intensive Care Units.

Key messages

- Quantitative lung analysis performed on low dose CT scans is accurate.

- Effective dose can be reduced up to 70% with minimal effects on quantitative results.

- If multiple chest CT scans are performed in order to characterize quantitatively the lung and assess the response to the application of different airway pressures (potential for lung recruitment), low dose CT can be used to reduce patient's radiation exposure.

- The use of ultra-low dose CT increases image noise significantly and reduces the accuracy of lung quantitative analysis.

Abbreviations

CT: computed tomography; ARDS: acute respiratory distress syndrome; mAs: tube current-time product; qCT: quantitative computed tomography; HU: Hounsfield units; $CTDI_{vol}$: volumetric computed tomography dose index; DLP: dose length product; E: effective dose; SD: standard deviation; kVp: peak tube voltage.

Authors' contributions

VV, TL and AIB conceived the study, performed the experiments, analyzed data and wrote the manuscript. VV and TL processed CT images and performed quantitative analysis. MB, CR, KKC, LCC, LG participated in study design, critically revised the manuscript, read and approved the final version of the manuscript.

Competing interests: The authors declare that they have no competing interests.

References

1. Goodman LR, Fumagalli R, Tagliabue P, Tagliabue M, Ferrario M, Gattinoni L, Pesenti A: **Adult respiratory distress syndrome due to pulmonary and extrapulmonary causes: CT, clinical, and functional correlations.** *Radiology* 1999, **213:**545-552.

2. Gattinoni L, Bombino M, Pelosi P, Lissoni A, Pesenti A, Fumagalli R, Tagliabue M: **Lung structure and function in different stages of severe adult respiratory distress syndrome.** *JAMA* 1994, **271:**1772-1779.

3. Gattinoni L, Caironi P, Pelosi P, Goodman LR: **What has computed tomography taught us about the acute respiratory distress syndrome?** *Am J Respir Crit Care Med* 2001, **164:**1701-1711.

4. Crotti S, Mascheroni D, Caironi P, Pelosi P, Ronzoni G, Mondino M, Marini JJ, Gattinoni L: **Recruitment and derecruitment during acute respiratory failure: a clinical study.** *Am J Respir Crit Care Med* 2001, **164:**131-140.

5. Malbouisson LM, Busch CJ, Puybasset L, Lu Q, Cluzel P, Rouby JJ: **Role of the heart in the loss of aeration characterizing lower lobes in acute respiratory distress syndrome. CT Scan ARDS Study Group.** *Am J Respir Crit Care Med* 2000, **161:**2005-2012.

6. Malbouisson LM, Muller JC, Constantin JM, Lu Q, Puybasset L, Rouby JJ: **Computed tomography assessment of positive end-expiratory pressure-induced alveolar recruitment in patients with acute respiratory distress syndrome.** *Am J Respir Crit Care Med* 2001, **163:**1444-1450.

7. Gattinoni L, Caironi P, Cressoni M, Chiumello D, Ranieri VM, Quintel M, Russo S, Patroniti N, Cornejo R, Bugedo G: **Lung recruitment in patients with the acute respiratory distress syndrome.** *N Engl J Med* 2006, **354:**1775-1786.

8. Caironi P, Cressoni M, Chiumello D, Ranieri M, Quintel M, Russo SG, Cornejo R, Bugedo G, Carlesso E, Russo R et al.: **Lung opening and closing during ventilation of acute respiratory distress syndrome.** *Am J Respir Crit Care Med* 2010, **181:**578-586.

9. Terragni PP, Rosboch G, Tealdi A, Corno E, Menaldo E, Davini O, Gandini G, Herrmann P, Mascia L, Quintel M et al.: **Tidal hyperinflation during low tidal volume ventilation in acute respiratory distress syndrome.** *Am J Respir Crit Care Med* 2007, **175:**160-166.

10. Pearce MS, Salotti JA, Little MP, McHugh K, Lee C, Kim KP, Howe NL, Ronckers CM, Rajaraman P, Sir Craft AW et al.: **Radiation exposure from CT scans in childhood and subsequent risk of leukaemia and brain tumours: a retrospective cohort study.** *Lancet* 2012, **380:**499-505.

11. Sarma A, Heilbrun ME, Conner KE, Stevens SM, Woller SC, Elliott CG: **Radiation and Chest CT Scan Examinations: What Do We Know?** *Chest* 2012, **142:**750-760.

12. Sodickson A, Baeyens PF, Andriole KP, Prevedello LM, Nawfel RD, Hanson R, Khorasani R: **Recurrent CT, cumulative radiation exposure, and associated radiation-induced cancer risks from CT of adults.** *Radiology* 2009, **251:**175-184.

13. Ravenel JG, Scalzetti EM, Huda W, Garrisi W: **Radiation exposure and image quality in chest CT examinations.** *AJR Am J Roentgenol* 2001, **177:**279-284.

14. Huda W: **Dose and image quality in CT.** *Pediatr Radiol* 2002, **32:**709-713.

15. Batchinsky AI, Jordan BS, Necsoiu C, Dubick MA, Cancio LC: **Dynamic changes in shunt and ventilation-perfusion mismatch following experimental pulmonary contusion.** *Shock* 2010, **33:**419-425.

16. Formenti P, Graf J, Santos A, Gard KE, Faltesek K, Adams AB, Dries DJ, Marini JJ: **Non-pulmonary factors strongly influence the stress index.** *Intensive Care Med* 2011, **37:**594-600.

17. Yuan R, Hogg JC, Pare PD, Sin DD, Wong JC, Nakano Y, McWilliams AM, Lam S, Coxson HO: **Prediction of the rate of decline in FEV(1) in smokers using quantitative Computed Tomography.** *Thorax* 2009, **64:**944-949.

18. Dambrosio M, Roupie E, Mollet JJ, Anglade MC, Vasile N, Lemaire F, Brochard L: **Effects of positive end-expiratory pressure and different tidal volumes on alveolar recruitment and hyperinflation.** *Anesthesiology* 1997, **87:**495-503.

19. Aberle DR, Adams AM, Berg CD, Black WC, Clapp JD, Fagerstrom RM, Gareen IF, Gatsonis C, Marcus PM, Sicks JD: **Reduced lung-cancer mortality with low-dose computed tomographic screening.** *N Engl J Med* 2011, **365:**395-409.

20. Church TR, Black WC, Aberle DR, Berg CD, Clingan KL, Duan F, Fagerstrom RM, Gareen IF, Gierada DS, Jones GC et al.: **Results of initial low-dose computed tomographic screening for lung cancer.** *N Engl J Med* 2013, **368:**1980-1991.

21. Dohan A, Soyer P: **Low-dose abdominal CT for diagnosing appendicitis.** *N Engl J Med* 2012, **367:**477-479.

22. Madani A, de M, V, Zanen J, Gevenois PA: **Pulmonary emphysema: radiation dose and section thickness at multidetector CT quantification--comparison with macroscopic and microscopic morphometry.** *Radiology* 2007, **243:**250-257.

23. Zompatori M, Fasano L, Mazzoli M, Sciascia N, Cavina M, Pacilli AM, Paioli D: **Spiral CT evaluation of pulmonary emphysema using a low-dose technique.** *Radiol Med* 2002, **104:**13-24.

24. Nishio M, Matsumoto S, Ohno Y, Sugihara N, Inokawa H, Yoshikawa T, Sugimura K: **Emphysema quantification by low-dose CT: potential impact of adaptive iterative dose reduction using 3D processing.** *AJR Am J Roentgenol* 2012, **199:**595-601.

25. Hirschl RB, Parent A, Tooley R, McCracken M, Johnson K, Shaffer TH, Wolfson MR, Bartlett RH: **Liquid ventilation improves pulmonary function, gas exchange, and lung injury in a model of respiratory failure.** *Ann Surg* 1995, **221:**79-88.

26. Kim JE, Newman B: **Evaluation of a radiation dose reduction strategy for pediatric chest CT.** *AJR Am J Roentgenol* 2010, **194:**1188-1193.

27. Wildberger JE, Mahnken AH, Schmitz-Rode T, Flohr T, Stargardt A, Haage P, Schaller S, Gunther RW: **Individually adapted examination protocols for reduction of radiation exposure in chest CT.** *Invest Radiol* 2001, **36:**604-611.

28. Rouby JJ, Puybasset L, Nieszkowska A, Lu Q: **Acute respiratory distress syndrome: lessons from computed tomography of the whole lung.** *Crit Care Med* 2003, **31:**S285-S295.

29. Huda W, Magill D, He W: **CT effective dose per dose length product using ICRP 103 weighting factors.** *Med Phys* 2011, **38:**1261-1265.

30. Wintermark M, Maeder P, Verdun FR, Thiran JP, Valley JF, Schnyder P, Meuli R: **Using 80 kVp versus 120 kVp in perfusion CT measurement of regional cerebral blood flow.** *AJNR Am J Neuroradiol* 2000, **21:**1881-1884.

31. Bland JM, Altman DG: **Statistical methods for assessing agreement between two methods of clinical measurement.** *Lancet* 1986, **1:**307-310.

32. Diederich S, Lenzen H: **Radiation exposure associated with imaging of the chest: comparison of different radiographic and computed tomography techniques.** *Cancer* 2000, **89:**2457-2460.

33. Reske AW, Busse H, Amato MB, Jaekel M, Kahn T, Schwarzkopf P, Schreiter D, Gottschaldt U, Seiwerts M: **Image reconstruction affects computer tomographic assessment of lung hyperinflation.** *Intensive Care Med* 2008, **34:**2044-2053.

34. Yuan R, Mayo JR, Hogg JC, Pare PD, McWilliams AM, Lam S, Coxson HO: **The effects of radiation dose and CT manufacturer on measurements of lung densitometry.** *Chest* 2007, **132:**617-623.

35. **FDA public health notification: reducing radiation risk from computed tomography for pediatric and small adult patients.** *Pediatr Radiol* 2002, **32:**314-316.

36. Newman B, Callahan MJ: **ALARA (as low as reasonably achievable) CT 2011--executive summary.** *Pediatr Radiol* 2011, **41 Suppl 2:**453-455.

37. Reske AW, Reske AP, Gast HA, Seiwerts M, Beda A, Gottschaldt U, Josten C, Schreiter D, Heller N, Wrigge H et al.: **Extrapolation from ten sections can make CT-based quantification of lung aeration more practicable.** *Intensive Care Med* 2010, **36:**1836-1844.

38. Reske AW, Rau A, Reske AP, Koziol M, Gottwald B, Alef M, Ionita JC, Spieth PM, Hepp P, Seiwerts M et al.: **Extrapolation in the analysis of lung aeration by computed tomography: a validation study.** *Crit Care* 2011, **15:**R279.

39. Yoshimura N, Sabir A, Kubo T, Lin PJ, Clouse ME, Hatabu H: **Correlation between image noise and body weight in coronary CTA with 16-row MDCT.** *Acad Radiol* 2006, **13:**324-328.

Table 1. Comparison between qCT results obtained at 60 and 140 mAs.

60 mAs – 140 mAs		Mean±SD$_{60}$	Mean±SD$_{140}$	p	r^2	Bias	LOA
BASELINE (n=12)	Lung volume [ml]	2782±666	2785±671	0.88	0.99	1.7	-114.0 – 109.0
	Lung tissue mass [g]	679±102	683±101	0.12	1.00	-4.5	-13.2 – 4.2
	Hyperinflated tissue [%]	0.6±1.1	0.5±1.0	0.08	0.97	0.1	-0.4 – 0.5
	Normally aerated tissue [%]	86.6±2.9	86.4±3.2	0.52	0.95	0.2	-1.7 – 2.1
	Poorly aerated tissue [%]	11.5±3.4	11.8±3.7	0.21	0.95	-0.3	-2.0 – 1.3
	Non aerated tissue [%]	1.4±0.5	1.3±0.7	0.07	0.98	0.1	-0.1 – 0.2
ARDS (n=28)	Lung volume [ml]	2022±338	2023±343	0.91	0.99	-0.7	-64.3 – 62.8
	Lung tissue mass [g]	1500±159	1498±151	0.73	0.98	1.8	-51.4 – 55.0
	Hyperinflated tissue [%]	0.0±0.1	0.0±0.1	0.52	0.95	0.0	-0.1 – 0.1
	Normally aerated tissue [%]	11.4±11.1	11.4±11.1	0.91	0.99	0.0	-2.4 – 2.4
	Poorly aerated tissue [%]	33.1±15.6	33.2±16.0	0.72	0.98	0.0	-4.5 – 4.4
	Non aerated tissue [%]	55.4±23.2	55.4±23.5	0.99	0.99	0.0	-5.5 – 5.5

Table 1. *Definition of abbreviations:* Lung volume = total lung volume; Lung tissue mass = total mass of lung tissue; Hyperinflated tissue = mass of hyperinflated tissue; Normally aerated tissue = mass of normally aerated tissue; Poorly aerated tissue = mass of poorly aerated tissue; Non aerated tissue = mass of non aerated tissue; p = p-value of the comparison between values obtained at 60 and at 140 mAs (paired t-test or Signed Rank Sum test as appropriate); r^2 = coefficient of determination of linear regressions between values obtained at 60 and at 140 mAs; bias and LOA = bias and limits of agreement (bias ± 1.96 SD) of the Bland-Altman analysis.

Table 2. Comparison between qCT results obtained at 60 and 15 mAs.

60 mAs – 15 mAs		Mean±SD$_{60}$	Mean±SD$_{15}$	p	r^2	Bias	LOA
BASELINE (n=18)	Lung volume [ml]	3227±1015	3224±995	0.80	1.0	3.4	-112.0 – 118.8
	Lung tissue mass [g]	711±128	707±129	0.17	0.99	4.3	-21.8 – 30.4
	Hyperinflated tissue [%]	3.3±5.5	3.9±5.6	<0.001	0.99	-0.7	-1.8 – 0.5
	Normally aerated tissue [%]	81.4±7.5	81.1±6.6	0.22	0.93	0.3	-4.2 – 4.8
	Poorly aerated tissue [%]	13.3±6.2	12.9±6.2	0.84	0.91	0.4	-3.3 – 4.1
	Non aerated tissue [%]	2.1±1.4	2.1±1.5	0.04	0.96	-0.1	-0.6 – 0.5
ARDS (n=18)	Lung volume [ml]	2295±561	2264±526	0.07	0.99	31.4	-105.8 – 168.6
	Lung tissue mass [g]	1778±315	1775±301	0.78	0.98	3.0	-85.1 – 91.1
	Hyperinflated tissue [%]	0.1±0.2	0.2±0.2	0.008	0.94	0.0	-0.1 – 0.1
	Normally aerated tissue [%]	9.3±9.7	8.8±9.4	0.13	0.98	0.5	-2.1 – 3.2
	Poorly aerated tissue [%]	28.1±13.4	28.6±12.6	0.44	0.96	-0.5	-4.8 – 3.9
	Non aerated tissue [%]	62.5±21.2	62.5±20.0	0.98	0.98	0.0	-6.9 – 6.9

Table 2. *Definition of abbreviations:* Lung volume = total lung volume; Lung tissue mass = total mass of lung tissue; Hyperinflated tissue = mass of hyperinflated tissue; Normally aerated tissue = mass of normally aerated tissue; Poorly aerated tissue = mass of poorly aerated tissue; Non aerated tissue = mass of non aerated tissue; p = p-value of the comparison between values obtained at 60 and at 15 mAs (paired t-test or Signed Rank Sum test as appropriate); r^2 = coefficient of determination of linear regressions between values obtained at 60 and at 15 mAs; bias and LOA = bias and limits of agreement (bias ± 1.96 SD) of the Bland-Altman analysis.

Table 3. Comparison between qCT results obtained at 60 and 7.5 mAs.

60 mAs – 7.5 mAs		Mean±SD$_{60}$	Mean±SD$_{7.5}$	p	r^2	Bias	LOA
BASELINE (n=16)	Lung volume [ml]	3180±1096	3162±1083	0.18	1.0	17.7	-87.9 – 123.3
	Lung tissue mass [g]	726±106	716±111	0.12	0.96	9.8	-39.2 – 58.8
	Hyperinflated tissue [%]	2.7±4.0	4.2±4.7	<0.001	0.94	-1.5	-4.1 – 1.1
	Normally aerated tissue [%]	81.9±7.1	79.6±5.6	0.002	0.90	2.3	-2.9 – 7.6
	Poorly aerated tissue [%]	13.4±6.9	14.1±6.4	0.50	0.88	-0.7	-5.4 – 3.9
	Non aerated tissue [%]	2.1±1.4	2.2±1.3	0.09	0.98	-0.1	-0.5 – 0.3
ARDS (n=17)	Lung volume [ml]	2321±499	2281±478	0.01	0.99	40.4	-73.8 – 154.6
	Lung tissue mass [g]	1807±286	1797±295	0.41	0.97	10.0	-86.1 – 106.1
	Hyperinflated tissue [%]	0.0±0.0	0.1±0.0	0.004	0.79	0.0	-0.1 – 0.0
	Normally aerated tissue [%]	9.1±9.5	8.7±9.1	0.20	0.98	0.4	-2.1 – 3.0
	Poorly aerated tissue [%]	27.3±13.7	30.2±11.3	0.008	0.95	-2.9	-10.5 – 4.8
	Non aerated tissue [%]	63.5±21.4	61.1±18.8	0.03	0.97	2.4	-5.9 – 10.8

Table 3 *Definition of abbreviations:* Lung volume = total lung volume; Lung tissue mass = total mass of lung tissue; Hyperinflated tissue = mass of hyperinflated tissue; Normally aerated tissue = mass of normally aerated tissue; Poorly aerated tissue = mass of poorly aerated tissue; Non aerated tissue = mass of non aerated tissue; p = p-value of the comparison between values obtained at 60 and at 7.5 mAs (paired t-test or Signed Rank Sum test as appropriate); r^2 = coefficient of determination of linear regressions between values obtained at 60 and at 7.5 mAs; bias and LOA = bias and limits of agreement (bias ± 1.96 SD) of the Bland-Altman analysis.

Table 4. Dose and noise evaluation

mAs	140	60	15	7.5	p
CTDI$_{vol}$ [mGy]	22.1±0.0	9.2±0.8	2.2±0.3	1.1±0.1	<0.001
DLP [mGy.cm]	870.5±47.7	362.2±45.2	96.5±39.0	44.9±6.4	<0.001
E [mSv]	17.8±1.0	7.4±0.9	2.0±0.8	0.9±0.1	<0.001
Image noise [HU]	10.0±1.1	15.9±3.5	37.5±10.6	73.8±17.5	<0.001

Table 4. *Definition of abbreviations:* CTDI$_{vol}$ = volumetric computed tomography dose index; DLP = dose length product; E = effective dose; Image noise = image noise of each applied mAs calculated as the mean standard deviation of tissue density (expressed in HU) of ten regions of interest placed on a uniform tissue (aorta) in ten different scans; p = p-value of the one way analysis of variance. Data are expressed as mean ± SD.

Figure legends

Figure 1.

Lung CT images of a sheep with ARDS induced by oleic acid. Images show the change in image quality due to the different current-time products (mAs) applied. Panel **A**: 140 mAs; Panel **B**: 60 mAs; Panel **C**: 15 mAs; Panel **D**: 7.5 mAs. Despite an increased image noise, the interface between lung and surrounding structures can be easily recognized.

Figure 2

Bland-Altman analysis of poorly and non aerated lung tissue for CT scans performed at 60 and 7.5 mAs after the induction of ARDS.

Definition of abbreviations: M_{poor} = poorly aerated mass; M_{non} = non aerated mass. All masses are expressed as percentage of total lung mass of tissue. Values on the X-axis represent the average between values recorded with two mAs, e.g., Mean Mpoor = (Mpoor CT_{60}+Mpoor $CT_{7.5}$)/2. Poorly aerated mass (**Panel A**): slope = 0.20, r^2 = 0.39, p = 0.01. Non aerated volume (**Panel B**): slope = 0.13, r^2 = 0.35, p = 0.01.

Figure 3.

Mean frequency distribution of CT numbers of scans performed at baseline (healthy lungs) expressed as percentage of tissue mass and grouped into intervals of 50 HU. Data are presented as mean ± standard error. Panel **A**: comparison between 60 and 140 mAs. Panel **B**: comparison between 60 and 15 mAs. Panel **C**: comparison between 60 and 7.5 mAs. * $p < 0.05$ *vs.* 60 mAs; paired t-test or Rank Sum Test, as appropriate. Vertical dashed lines delimitate lung compartments as defined in the *Materials and methods*.
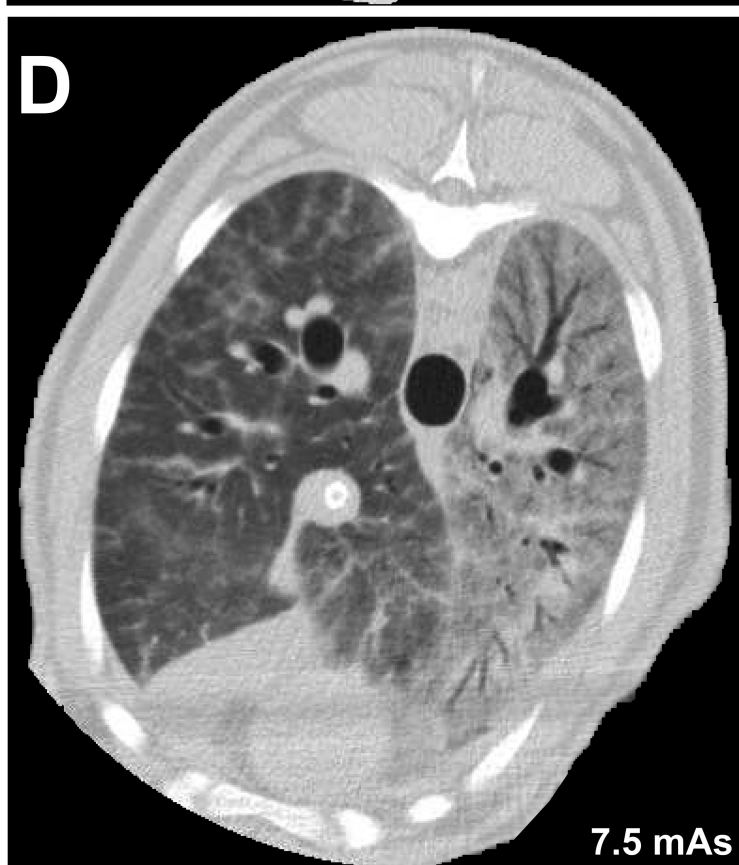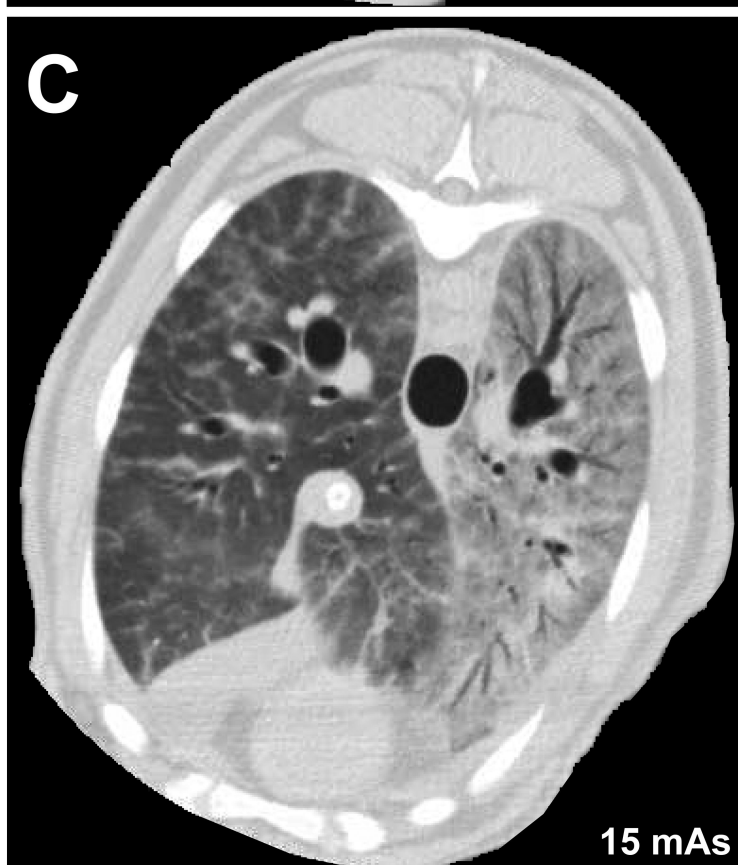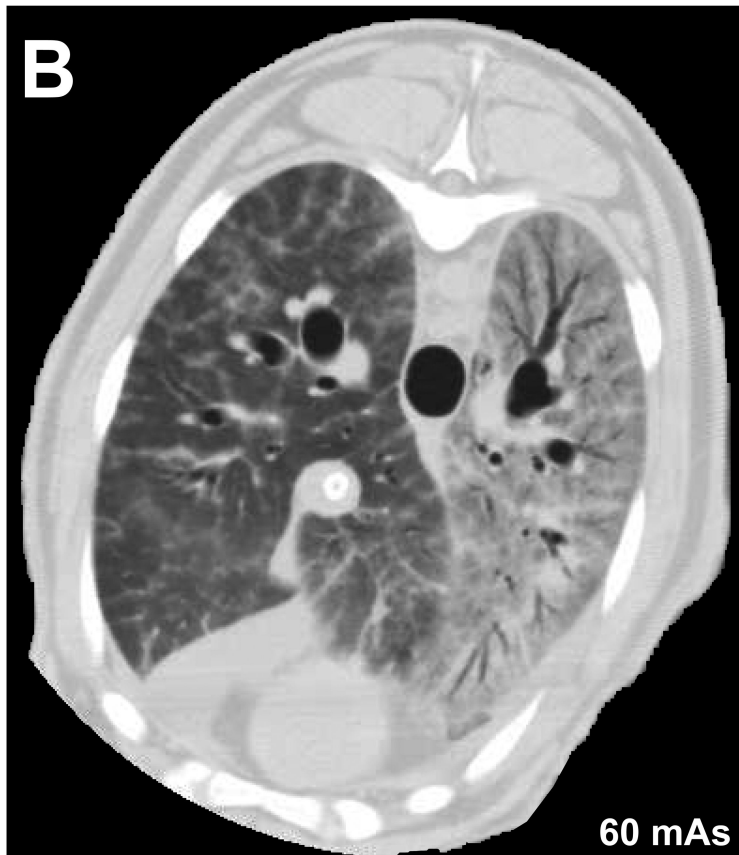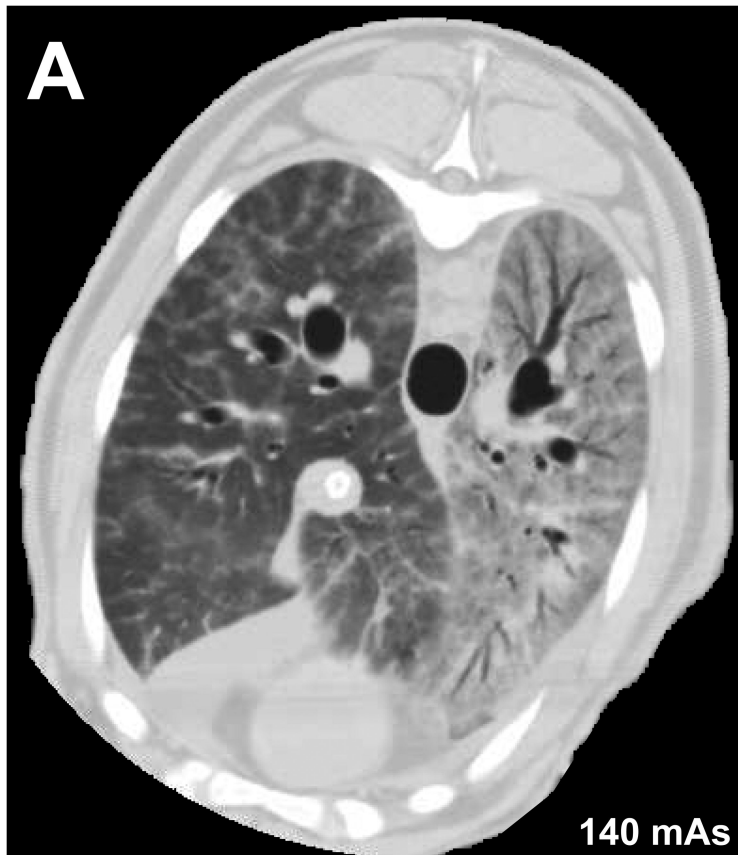
Figure 4.

Mean frequency distribution of CT numbers of scans performed on sheep with experimental ARDS expressed as percentage of tissue mass and grouped into intervals of 50 HU. Data are presented as mean ± standard error. Panel **A**: comparison between 60 and 140 mAs. Panel **B**: comparison between 60 and 15 mAs. Panel **C**: comparison between 60 and 7.5 mAs. * $p < 0.05$ *vs.* 60 mAs; paired t-test or Rank Sum Test, as appropriate. Vertical dashed lines delimitate lung compartments as defined in the *Materials and Methods*.
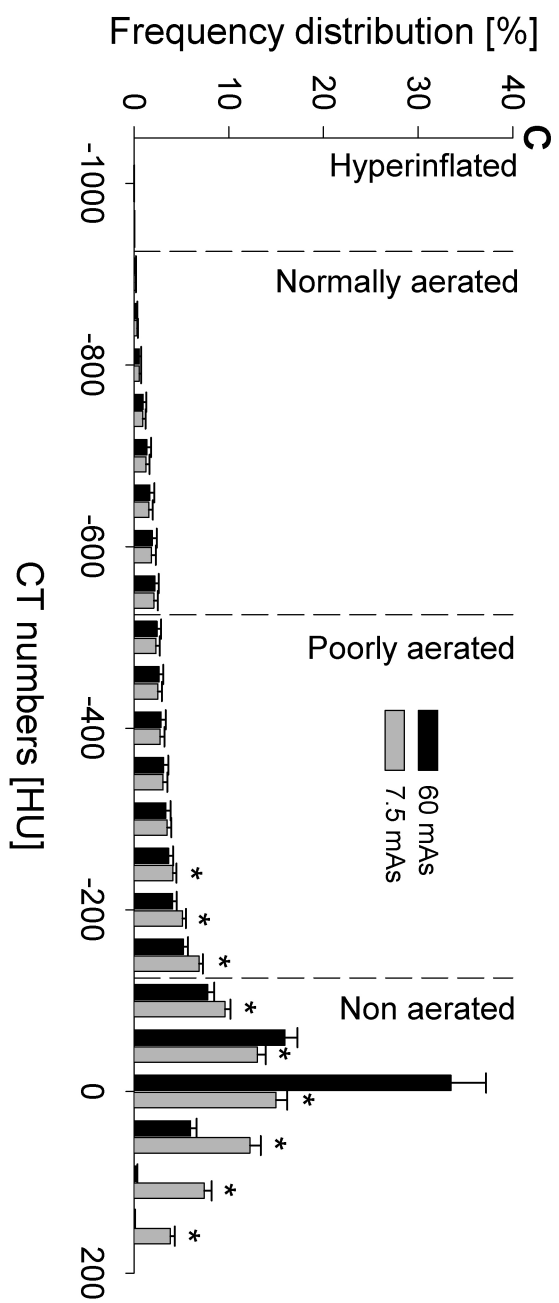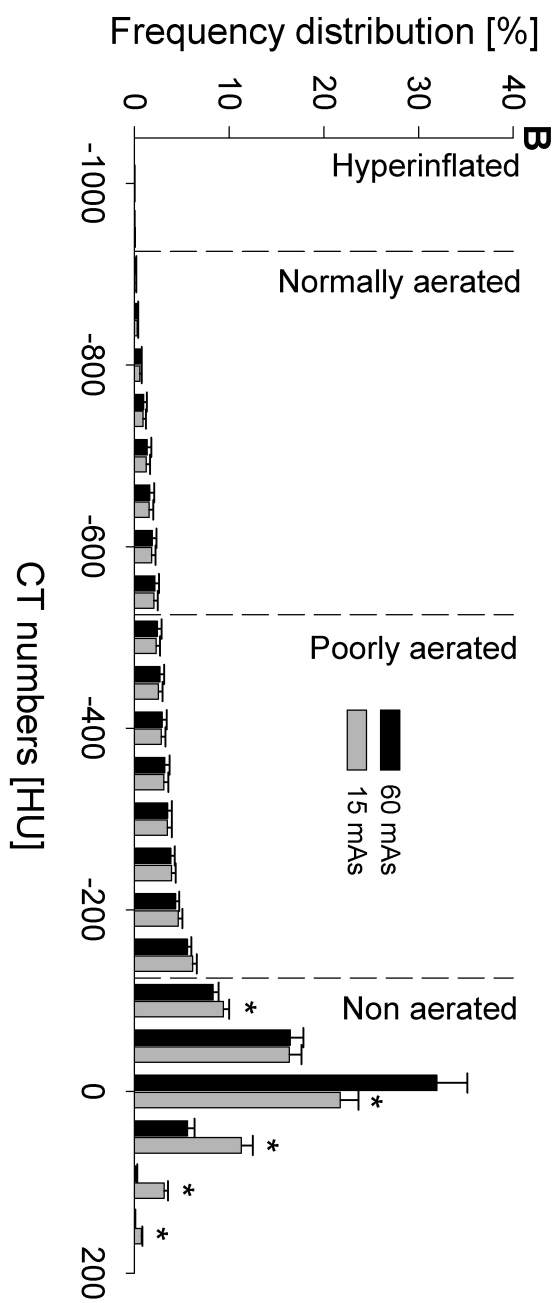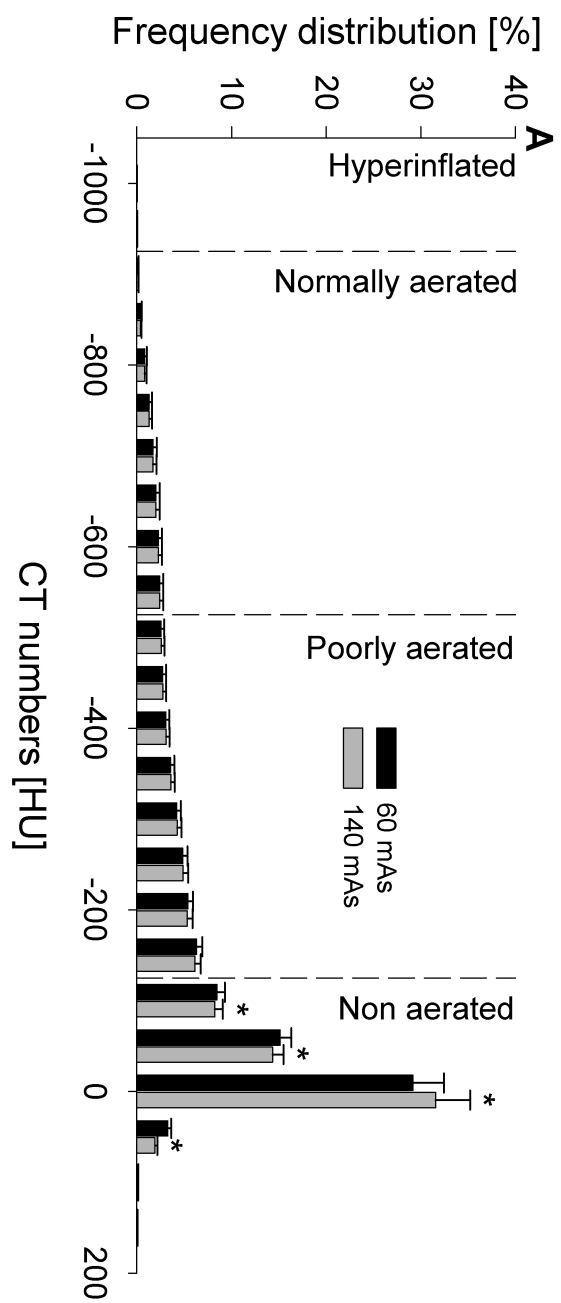
Figure 1
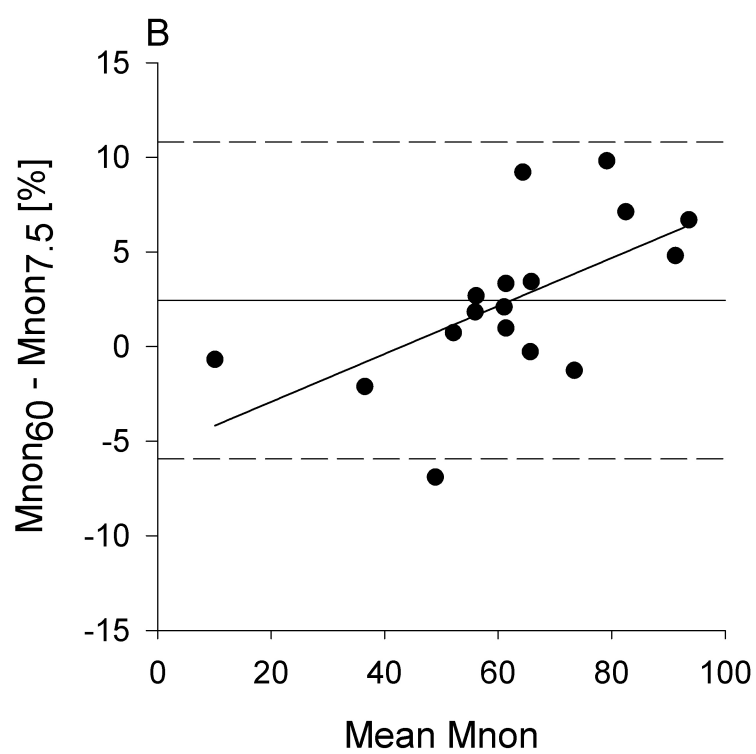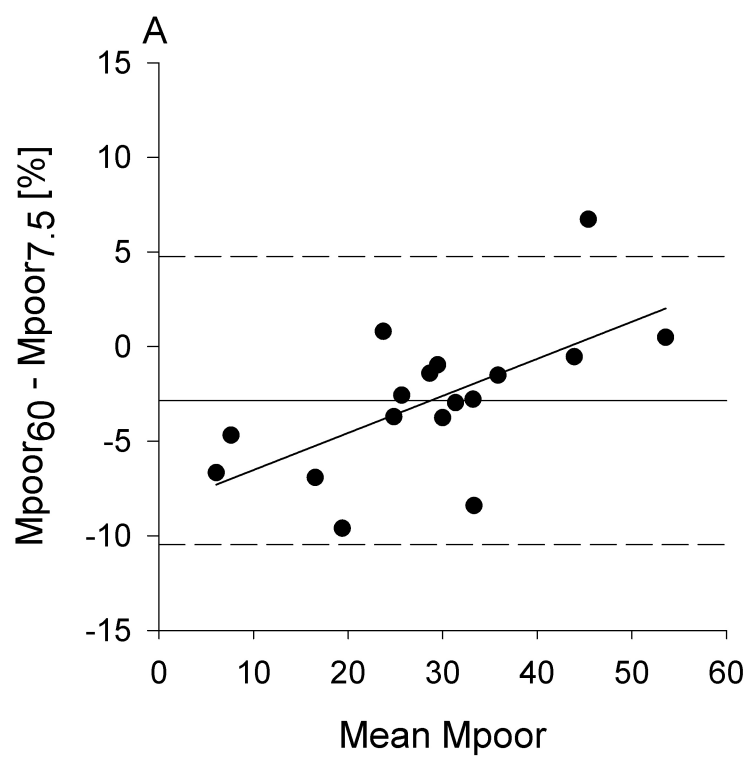
Figure 2

Figure 3

Figure 4
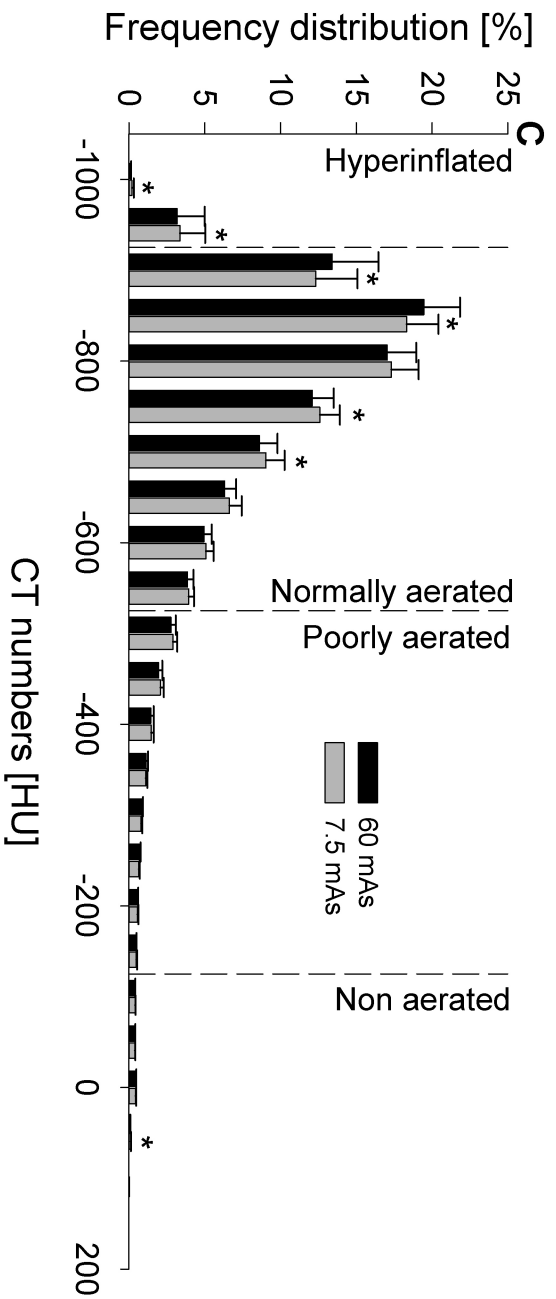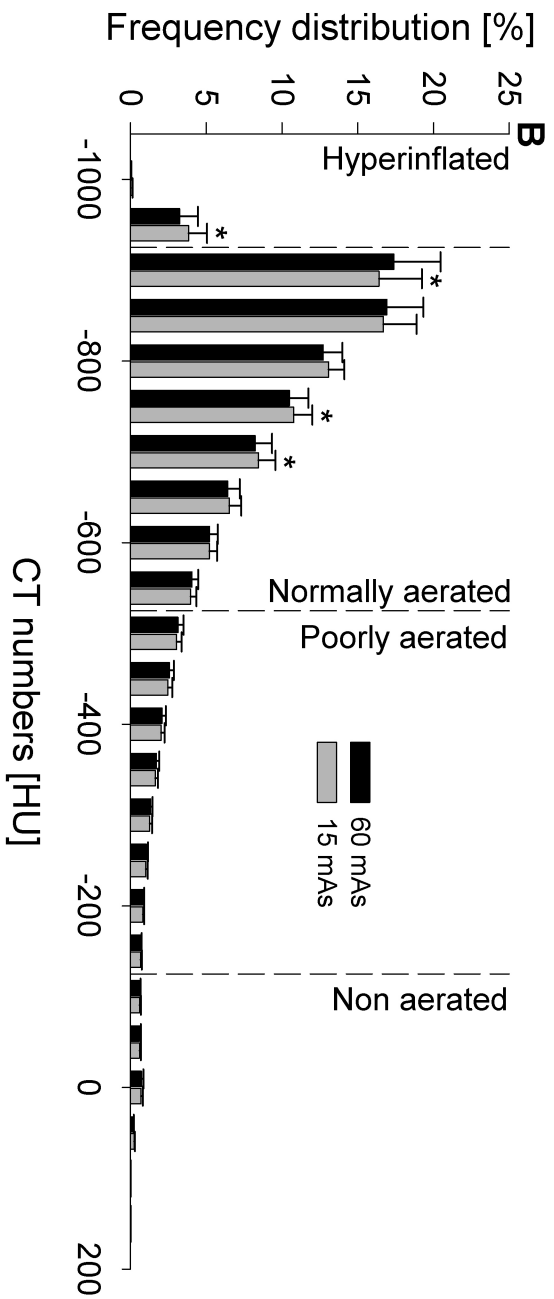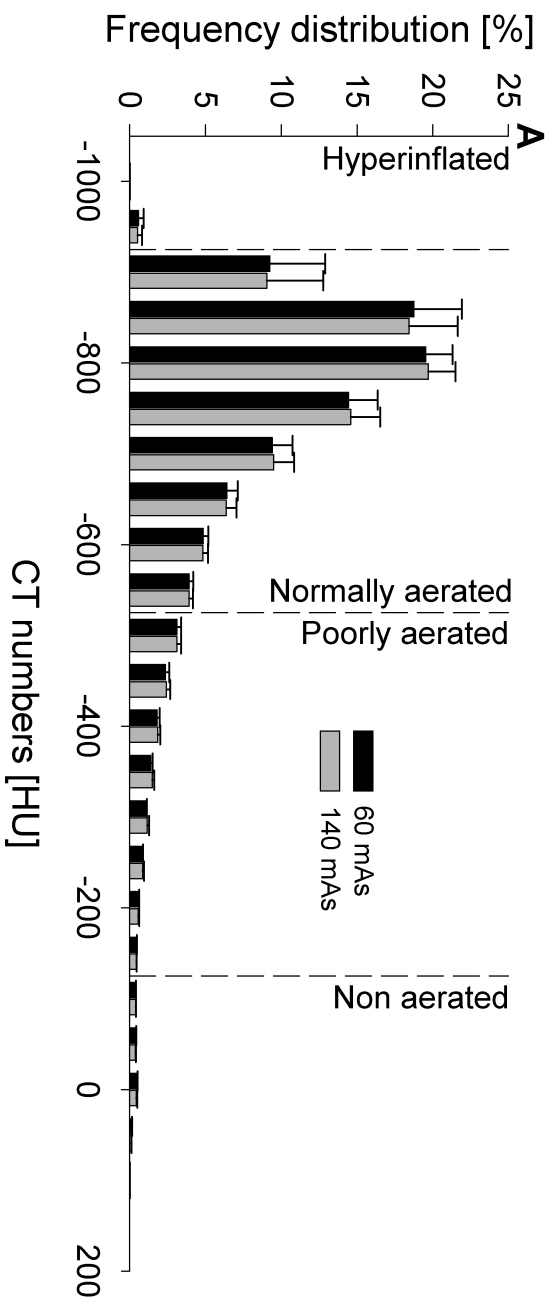
Additional files provided with this submission:

Additional file 1: Vecchi V_ElectronicSupplementaryMaterial.doc, 137K
http://ccforum.com/imedia/117809489104563/supp1.doc